Journal of Oral Biosciences 64 (2022) 85–92

Contents lists available at ScienceDirect

Journal of Oral Biosciences

journal homepage: www.elsevier.com/locate/job

Original Article

LPA_6-RhoA signals regulate junctional complexes for polarity and morphology establishment of maturation stage ameloblasts

Akira Inaba [a, b], Hidemitsu Harada [a], Shojiro Ikezaki [a], Mika Kumakami-Sakano [a], Haruno Arai [a, b], Marii Azumane [a, c], Hayato Ohshima [d], Kazumasa Morikawa [b], Kuniyuki Kano [e], Junken Aoki [e], Keishi Otsu [a, *]

[a] Division of Developmental Biology and Regenerative Medicine, Department of Anatomy, Iwate Medical University, 1-1-1, Idaidori, Yahaba, Iwate 028-3694, Japan
[b] Division of Pediatric and Special Care Dentistry, Department of Oral Health Science, School of Dentistry, Iwate Medical University, 19-1, Uchimaru, Morioka, Iwate 020-8505, Japan
[c] Division of Oral and Maxillofacial Surgery, Department of Reconstructive Oral and Maxillofacial Surgery, Iwate Medical University, 19-1, Uchimaru, Morioka, Iwate 020-8505, Japan
[d] Division of Anatomy and Cell Biology of the Hard Tissue, Department of Tissue Regeneration and Reconstruction, Niigata University Graduate School of Medical and Dental Sciences, 2-5274 Gakkocho-dori, Chuo-ku, Niigata 951-8514, Japan
[e] Department of Health Chemistry, Graduate School of Pharmaceutical Sciences, The University of Tokyo, 7-3-1, Bunkyo-ku, Hongo, Tokyo 113-0033, Japan

ARTICLE INFO

Article history:
Received 22 December 2021
Accepted 24 December 2021
Available online 21 January 2022

Keywords:
Ameloblast
Enamel
Cell adhesion molecules
Lysophosphatidic acid receptor
rhoA GTP-Binding protein

ABSTRACT

Objectives: Lysophosphatidic acid (LPA) is a potent bioactive phospholipid that exerts various functions upon binding to six known G protein-coupled receptors (LPA_{1-6}); however; its role in a tooth remains unclear. This study aimed to explore the impact of the LPA/LPA receptor 6 (LPA_6)/RhoA signaling axis on maturation stage ameloblasts (M-ABs), which are responsible for enamel mineralization.
Methods: The expression of LPA_6 and LPA-producing synthetic enzymes during ameloblast differentiation was explored through immunobiological analysis of mouse incisors and molars. To elucidate the role of LPA_6 in ameloblasts, incisors of LPA_6 KO mice were analyzed. *In vitro* experiments using ameloblast cell lines were performed to validate the function of LPA-LPA_6-RhoA signaling in ameloblasts.
Results: LPA_6 and LPA-producing enzymes were strongly expressed in M-ABs. In LPA_6 knockout mice, M-ABs exhibited abnormal morphology with the loss of cell polarity, and an abnormal enamel epithelium containing cyst-like structures was formed. Moreover, the expression of E-cadherin and zonula occludens-1 (ZO-1) significantly decreased in M-ABs. *In vitro* experiments demonstrated that LPA upregulated the expression of E-cadherin, ZO-1, and filamentous actin (F-actin) at the cellular membrane, whereas LPA_6 knockdown decreased their expression and changed cell morphology. Furthermore, we showed that RhoA signaling mediates LPA-LPA_6-induced junctional complexes.
Conclusions: This study demonstrated that LPA-LPA_6-RhoA signaling is essential for establishing proper cell morphology and polarity, via cell–cell junction and actin cytoskeleton expression and stability, of M-ABs. These results highlight the biological significance of bioactive lipids in a tooth, providing a novel molecular regulatory mechanism of ameloblasts.

1. Introduction

Lysophosphatidic acid (1- or 2-acyl-*sn*-glycerol-3-phosphate) is a bioactive phospholipid composed of one fatty acid chain and a polar phosphate group that is present in all eukaryotic tissues and blood plasma [1]. LPA can induce numerous cell-specific and context-dependent biological effects via G protein-coupled receptors [2,3]. To date, six differentially expressed receptors for LPA have been identified, of which, LPA_1, LPA_2, and LPA_3 belong to the endothelial differentiation gene family, and LPA_4, LPA_5, and LPA_6 belong to the P2Y family, which play important roles in various (patho)physiological conditions [4,5]. The LPA-LPA_6 axis was previously shown to regulate the differentiation and maturation of ectodermal appendages like hair follicles [6–10]. Homozygous mutations affecting the LPA-producing synthetic enzymes,

Abbreviations: IEE, inner enamel epithelial cell; LPA, lysophosphatidic acid; LPA_6, LPA receptor 6; M-AB, maturation stage ameloblast; S-AB, secretory stage ameloblast.

* Corresponding author. Fax: +81 19 908 8017.
E-mail address: kotsu@iwate-med.ac.jp (K. Otsu).

https://doi.org/10.1016/j.job.2022.01.004
1349-0079/

phosphatidic acid-preferring phospholipase A_1 (PA-PLA$_1\alpha$) and P2Y5/LPA$_6$, have been identified to cause congenital hair disorders, as well as misalignment of hair follicle epithelial cells, especially in Henle's layer. However, the involvement of the LPA-LPA$_6$ signaling in other ectodermal appendages, such as tooth, remains unclear.

The enamel covering of the tooth crown is the most highly mineralized tissue in the vertebrate body. During enamel formation or amelogenesis, ameloblasts, which are derived from oral epithelial cells of ectodermal origin, undergo multiple differentiation events associated with morphological and junctional changes. Inner enamel epithelial cells (IEEs) differentiate into secretory stage ameloblasts (S-ABs) that produce the enamel matrix proteins amelogenin and ameloblastin. These secretory cells then transform into maturation stage ameloblasts (M-ABs) that modulate enamel mineralization by controlling pH, transporting minerals, and modulating protein decomposition and absorption (Fig. 1A–D) [11]. These columnar M-ABs exhibit high polarity with a distinct distribution of junctional proteins and actin cytoskeleton that enables them to exert cell-specific functions [12], whereas the absence of their morphology and polarity can induce enamel malformation via enamel hypomineralization [13]. Therefore, elucidating the regulatory mechanism of M-ABs is indispensable for understanding normal enamel formation, as well as the etiology and pathophysiology of enamel hypomineralization. Nonetheless, such regulatory events of M-ABs remain largely unknown.

RhoA belongs to the Rho-family of small GTPases that function as molecular switches in a wide range of cellular processes [14]. RhoA activity is transduced by its downstream effectors, such as Rho-associated coiled-coil containing protein kinase that promotes the formation of tight junctions, adherens junctions [15], and actomyosin [16]. Recently, we demonstrated that RhoA signaling regulates dental epithelial stem cells and S-ABs by modulating the distinctive distribution of the junctional complex [17,18]. Furthermore, LPA$_6$ couples with Gα_{13} protein to activate RhoA signaling in hair follicles [10]. However, the role of RhoA signaling in M-ABs and its upstream regulator is yet to be elucidated.

In this study, using rodent tooth as the experimental model, we explored the molecular mechanism underlying LPA-mediated ameloblast regulation. LPA-LPA$_6$-RhoA signaling was found to be a modulator of cell morphology and polarity, via cell–cell junction and actin cytoskeleton expression and stability, of M-ABs. This novel regulatory mechanism of M-ABs provides a better understanding of enamel mineralization and further elucidates the pathogenesis of enamel hypomineralization.

2. Materials & methods

2.1. Animals and preparation of tissues

LPA$_6$ knockout (KO) mice with a mixed 129/Sv and C57BL/6 and their littermate control wild type (WT) mice were obtained from Deltagen (San Carlos, CA, USA). ddY mice (Japan SLC, Shizuoka, Japan) were used as the WT. For histological analysis, the mice were euthanized with CO_2 inhalation or cervical dislocation. The jaws were fixed in 4% paraformaldehyde and decalcified using Osteosoft (Merck, Darmstadt, Germany). For hematoxylin and eosin (H&E) staining and immunostaining, paraffin-embedded thin tissue sections (thickness, 6–7 μm) were used. All experiments were performed independently at least three times ($n = 3$) in triplicate where possible and when applicable.

2.2. Cell culture

Ameloblast cell lines HAT7 and mHAT9d were established from rat and mouse incisors, respectively, and cultured as described previously [19]. For analyzing the effect of LPA, cells were serum-starved for 18 h or transfected with LPA$_6$ small interference (si) RNA prior to the administration of LPA (Abcam, Cambridge, UK). Cells were treated with Y-27632 (Wako, Tokyo, Japan) and latrunculins A (LAT-A, Thermo Fisher Scientific, Waltham, MA, USA).

2.3. Immunohistochemistry, immunofluorescence, and elemental mapping by electron probe micro-analysis (EPMA)

Immunohistochemical and immunofluorescent staining were performed as described previously [17]. The antibodies used in this study are listed inTable S1. To detect filamentous actin (F-actin), cells were stained using Alexa Fluor 488- or 546-conjugated phalloidin (A12379, A22283; Thermo Fisher Scientific). Images were obtained using a fluorescence microscope (BX51, IX71; Olympus BZ-X800 Tokyo, Japan), laser-scanning confocal microscope (C1si; Nikon, Tokyo, Japan) or imaging cytometer (Cytell Cell Imaging System, GE Healthcare, Chicago, IL, USA). Image analyses were performed using ImageJ (https://imagej.nih.gov/ij/) or the software provided with the microscope. Appropriate positive and negative controls were run during each experiment. Elemental mapping of Ca, P, and Mg was performed by EPMA (EPMA-1610; Shimadzu, Kyoto, Japan) [20].

2.4. Small interfering RNA (siRNA)

siRNA transfection was performed as described previously [17]. Two sets of 25-mer duplex siRNA targeting genes and control siRNA were obtained from Thermo Fisher Scientific. All siRNA duplexes (10 nmol/L) were transfected into cells using Lipofectamine RNAiMAX (Thermo Fisher Scientific) for 48 h according to the manufacturer's protocol.

2.5. Quantitative reverse transcription-polymerase chain reaction (qRT-PCR)

Total RNA was extracted using RNeasy mini Kit (Qiagen, Hilden, Germany). Reverse transcription of total RNA was performed using PrimeScript RT reagent kit (Takara Bio, Kusatsu, Japan). Quantitative analysis of gene expression was performed by qRT-PCR using SYBR1 Premix Ex Taq (Takara Bio) and oligonucleotide primers specific for the target sequences (Table S2) on a Thermal Cycler Dice (Takara Bio) according to the manufacturer's protocol. Target gene levels were normalized against those of *Gapdh* using the comparative $2^{-\Delta\Delta Ct}$ method. Experiments were run in triplicate.

2.6. Statistical analyses

All data are reported as mean ± SEM. Differences were considered statistically significant if $p < 0.05$ using unpaired two-tailed Student's *t*-test. * and ** denote $p < 0.05$ and $p < 0.01$, respectively.

3. Results

3.1. LPA$_6$ and LPA-producing enzymes are distinctly expressed in maturation stage ameloblasts

Firstly, the expression of LPA$_6$ during ameloblast differentiation was determined through immunobiological analysis of mouse incisors and molars. On postnatal day 40 (P40), modest expression of LPA$_6$ was observed in the IEEs of upper incisors (Fig. 1E). In S-ABs, LPA$_6$ was uniformly expressed throughout the cytoplasm (Fig. 1F), whilst in M-ABs, high expression was observed at the basal and proximal ends in addition to the cytoplasm (Fig. 1G). In P1 molars, LPA$_6$ expression was observed in the S-AB cytoplasm, with modest

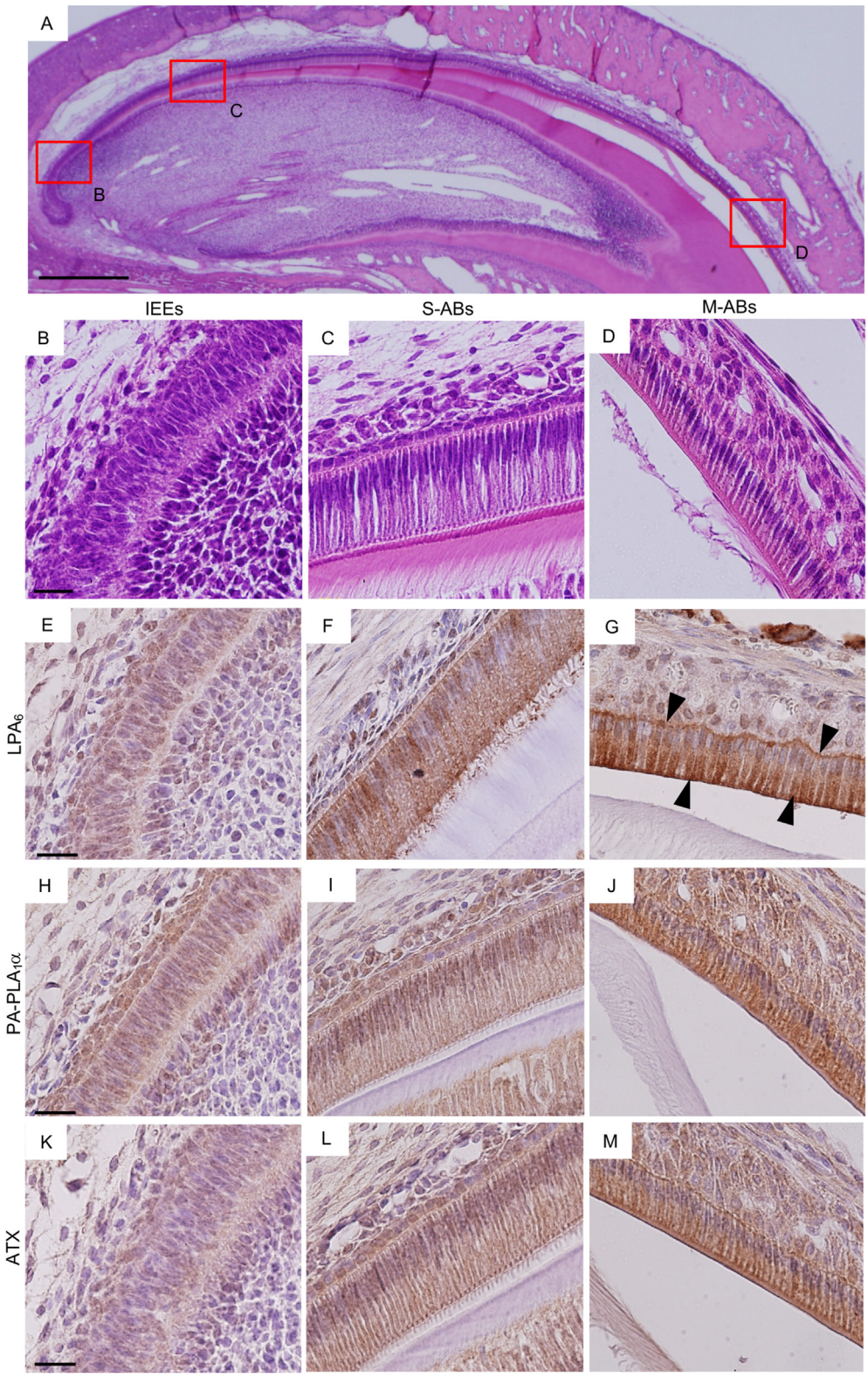

Fig. 1. LPA_6, $PA\text{-}PLA_1\alpha$ and ATX expression in mouse incisors. (A) Low magnification image of H&E-stained sections of P40 mouse maxillary incisors. The boxed areas in A are magnified in B-D. (B) Inner enamel epithelium cells. (C) Secretory stage ameloblasts. (D) Maturation stage ameloblasts. LPA_6 (E–G), $PA\text{-}PLA_1\alpha$ (H–J), and ATX (K–M) immunostaining of P40 mouse maxillary incisors. Scale bars: 500 μm (A); 20 μm (B–M).

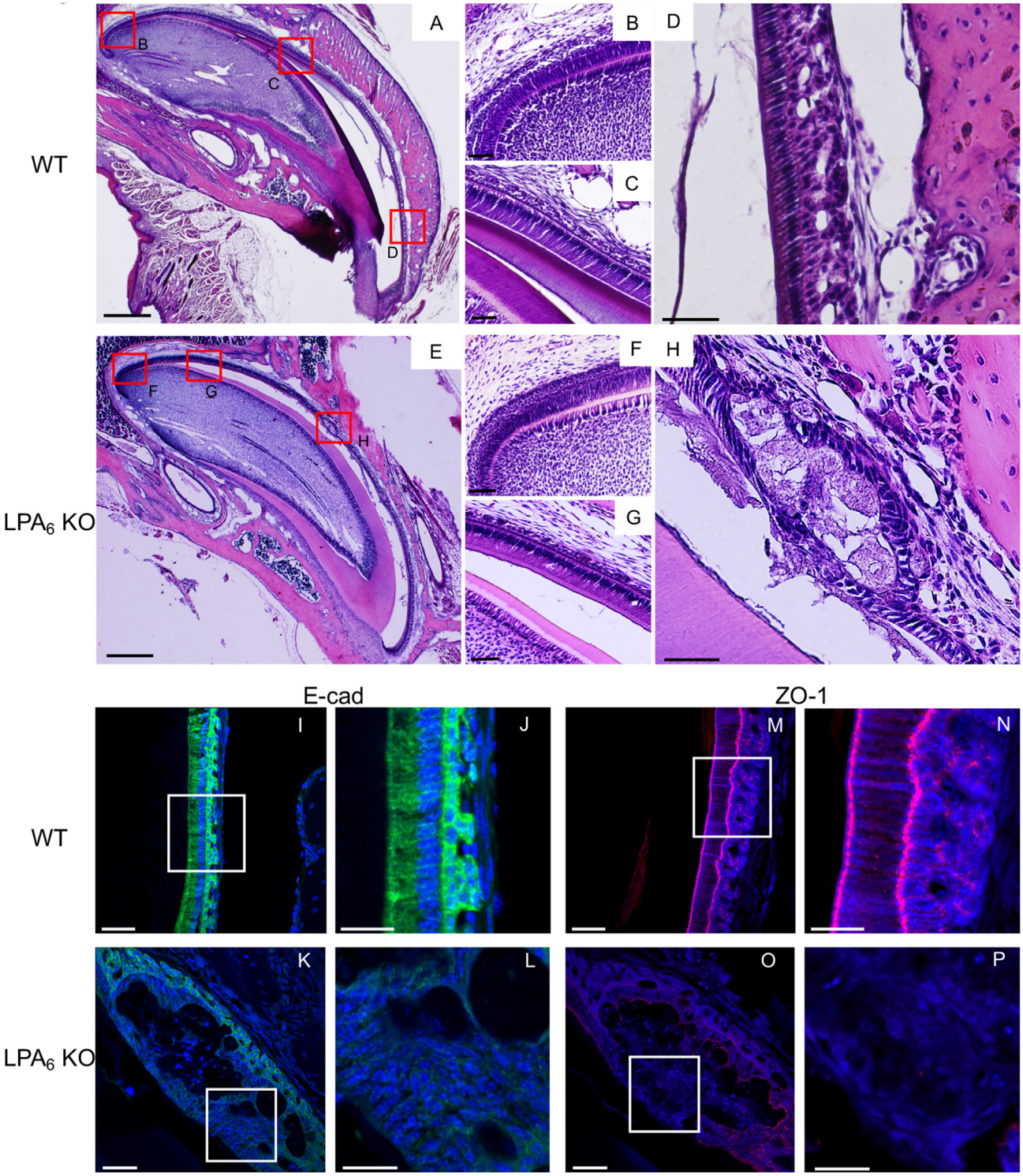

Fig. 2. Histological analysis of LPA_6 knockout mice. H&E staining of P40 WT (A–D) and LPA_6 KO (E–H) mouse maxillary incisors. The boxed areas in A and E are magnified in B-D and F–H, respectively. (I–L) E-cadherin staining of maturation stage ameloblasts in WT and LPA_6 KO mice. The boxed areas in I and K are magnified in J and L, respectively. (M–P) ZO-1 staining of maturation stage ameloblasts in WT and LPA_6 KO mouse maxillary incisors. The boxed areas in M and O are magnified in N and P, respectively. The nucleus is stained with DAPI (blue). Scale bars: 500 μm (A, E); 20 μm (B-D, F–H); 50 μm (I, K, M, O); 25 μm (J, L, N, P).

expression in IEEs of the cervical loop (Fig. S1A–D). In P9 molars, distinct expression of LPA_6 was observed at the basal and proximal end of M-ABs (Fig. S1E–G), whilst no detectable expression of LPA_6 was observed in the Hertwig epithelial sheath (Fig. S1E,H, arrowheads). Furthermore, the expression of LPA-producing synthetic enzymes, PA-$PLA_1\alpha$—a secreted membrane-associated protein concentrated on the plasma membrane [21]—and autotaxin (ATX)—a secreted glycoprotein that acts as lysophospholipase D,

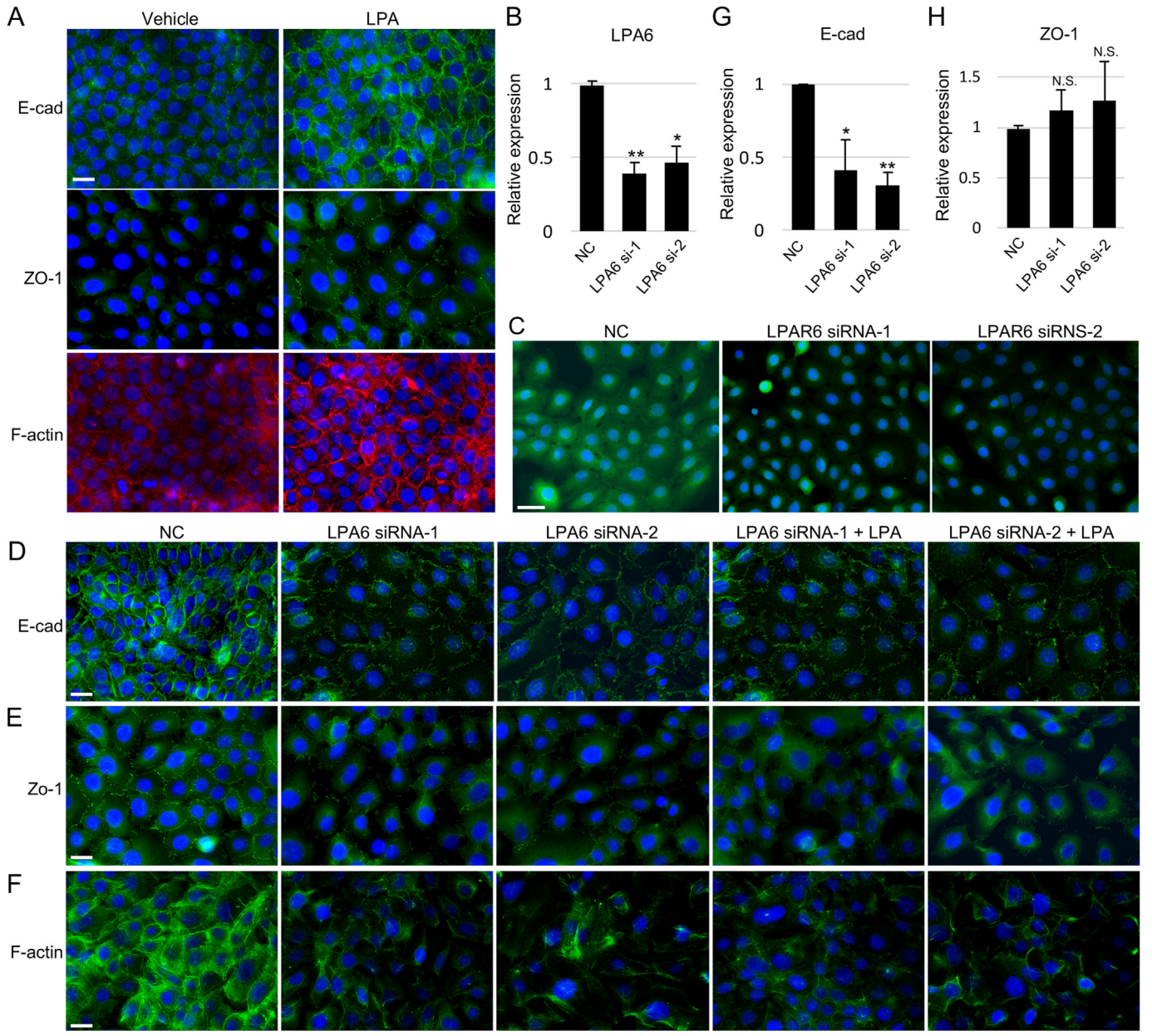

Fig. 3. The role of LPA-LPA$_6$ signaling in junctional proteins and actin cytoskeleton. (A) Immunostaining of E-cad and ZO-1, and Phalloidin staining (F-actin) in serum-starved HAT7 cells stimulated with vehicle (left) or LPA (20 μM, 24h) (right). (B) Expression of LPA$_6$ mRNA in HAT7 cells transfected with non-specific control siRNA (NC) or LPA$_6$-specific siRNA; $n = 4$. (C) Immunofluorescence of LPA$_6$ in HAT7 cells transfected with non-specific control siRNA (NC) or LPA$_6$-specific siRNA. Immunofluorescence of E-cad (D) and ZO-1 (E), and Phalloidin staining (F-actin) (F) in HAT7 cells transfected with NC siRNA, LPA$_6$-specific siRNA, and LPA$_6$-specific siRNA coupled with LPA treatment (20 μM, 24h). Expression of E-cad (G) and ZO-1 (H) mRNA in HAT7 cells transfected with non-specific control siRNA (NC) or LPA$_6$-specific siRNA; $n = 4$. Data are represented as their mean ± SEM. *$p < 0.05$, **$p < 0.01$, N.S.: not significant (unpaired two-tailed Student's *t*-test). Scale bars, 20 μm (A, C–F).

converting lysophosphatidylcholine into LPA [22]—was increased during ameloblast differentiation from IEEs to M-ABs in mouse incisors (Fig. 1H–M). Similar observation was reported during ameloblast differentiation in mouse molars (Fig. S2). Notably, PA-PLA$_1\alpha$ and ATX were strongly expressed in M-ABs (Fig. 2J,N).

3.2. Ameloblasts in LPA$_6$ knockout mice loose cell polarity and cell–cell adhesion

To further elucidate the role of LPA$_6$ during ameloblast differentiation, incisors of LPA$_6$ KO mice were analyzed. No obvious differences in the appearance and concentration of minerals (calcium, phosphorus, and magnesium) in EPMA analysis were reported in the incisor enamel and dentin compared to WT (data not shown). However, histological examination revealed abnormal morphology of M-ABs with the loss of cell polarity and cyst-like structures in part of the epithelium. The M-ABs and the papillary layer were indistinguishable, while IEE and S-ABs exhibited a normal appearance (Fig. 2A–H). Subsequently, the effect of LPA$_6$ deletion on cell–cell adhesion was analyzed due to its role in establishing cell polarity. In WT mice, E-cadherin (E-cad) was strongly expressed in M-ABs and the papillary layer (Fig. 2I and J),

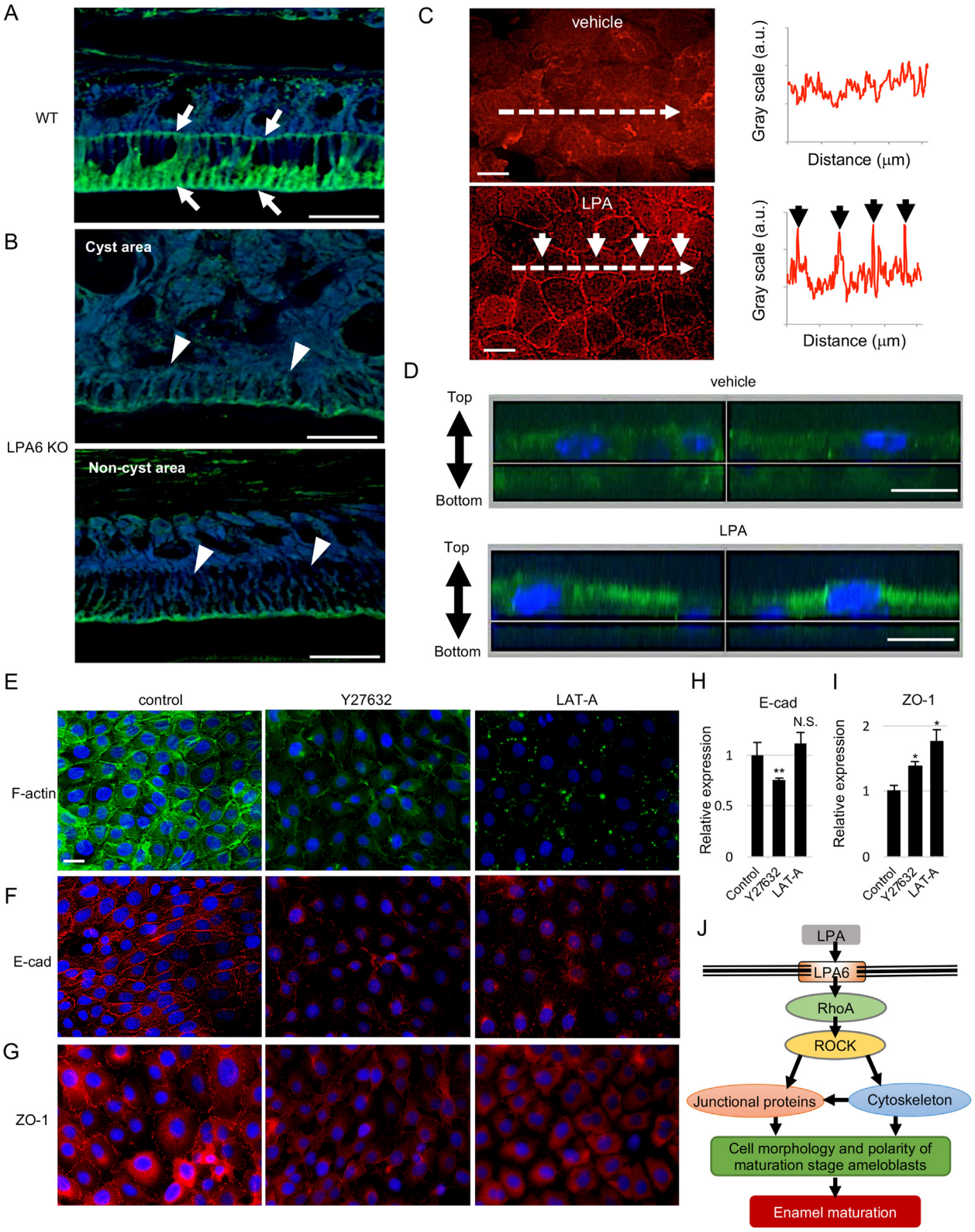

Fig. 4. RhoA mediated LPA_6-induced cell–cell adhesion and actin cytoskeleton. Immunostaining of active RhoA in maturation stage ameloblasts of WT (A) and LPA_6 KO mouse maxillary incisors (B, top; cyst forming area, bottom; non-cyst forming area). (C) Active RhoA staining of serum-starved mHAT9d cells treated with vehicle or LPA (20 μM). Line scan graphs show the active RhoA intensity along the white dotted line. (D) XZ image of active RhoA immunostained (green) mHAT9d cells treated with vehicle (top) and LPA (bottom). Phalloidin staining (F-actin) (E) and immunostaining for E-cad (F) and ZO-1 (G) of HAT7 cells after treatment with Y27632 (50 μM) or LAT-A (1 μM) for 24 h. Expression of E-cad (H) and ZO-1 (I) mRNA in HAT7 cells treated with Y27632 and LAT-A; $n = 4$. (J) Schematic of LPA_6 signaling mechanism involved in establishing cell polarity and morphology of M-ABs. Data are represented as their mean ± SEM. $*p < 0.05$, $**p < 0.01$, N.S.: not significant (unpaired two-tailed Student's *t*-test). Scale bars, 30 μm (A, B); 20 μm (E–G); 10 μm (C, D).

whilst ZO-1 expression was restricted to the distal and proximal ends of M-ABs (Fig. 2M,N). In contrast, E-cadherin and ZO-1 expression remarkably decreased in M-ABs of LPA_6 KO mice (Fig. 2K,L,O,P).

3.3. LPA-LPA_6 signaling contributes to cell–cell adhesion and actin cytoskeleton of ameloblasts in vitro

To validate the function of LPA-LPA_6 signaling in ameloblasts, we performed *in vitro* experiments using ameloblast cell lines. Firstly, we validated the effect of LPA on cell–cell adhesion and actin cytoskeleton. Administration of LPA up-regulated E-cad, ZO-1, and F-actin expression at the cellular membrane of both HAT7 cells and mHAT9d cells (Fig. 3A,Fig. S3). Additionally, on transfecting HAT7 with two different siRNAs specific for LPA_6, its expression was significantly reduced at both the mRNA and protein levels (Fig. 3B and C). Immunostaining demonstrated that E-cad and ZO-1 were expressed at the cellular membrane of WT cells, whereas their expression was fragmented and decreased in LPA_6 knocked down (KD) cells (Fig. 3D and E). F-actin expression was also remarkably reduced at the cellular membrane, generating cortical tension and thereby, influencing cell shape (Fig. 3F). Furthermore, the administration of LPA failed to recover E-cad, ZO-1, and F-actin expression in LPA_6 KD cells (Fig. 3D–F). qRT-PCR analysis indicated that knocking down LPA_6 decreased *E-cad* mRNA expression (Fig. 3G), but not ZO-1 (Fig. 3H).

3.4. LPA-LPA_6 signaling activates RhoA

We previously demonstrated that RhoA signaling regulated cell–cell adhesion and cytoskeleton in ameloblasts [17,23]. Therefore, we hypothesized that RhoA mediated the regulation of cell–cell adhesion and cell polarity of M-ABs via LPA-LPA_6 signaling. First, we compared the RhoA activation status in M-ABs between WT and LPA_6 KO mice. In LPA_6 KO mice, the expression of active RhoA (GTP-binding form) remarkably decreased, especially at the proximal end of M-ABs (Fig. 4B, arrow heads), compared to WT (Fig. 4A, arrows). Next, we examined whether RhoA activation was induced by LPA *in vitro*. Immunofluorescent data indicated that LPA administration increased active RhoA expression at the cellular cortex of mHAT9d cells (Fig. 4C). Three-dimensional images also revealed that active RhoA expression was induced at the side of M-ABs facing the culture media containing LPA (Fig. 4D). Finally, we analyzed Rho signaling and its downstream processes, actin polymerization, and E-cad and ZO-1 expression in HAT7 cells. First, we examined the effects of Rho signal inhibitor (Y27632) and actin polymerization inhibitor (LAT-A) on E-cad and ZO-1 at the protein level by immunofluorescent staining. Phalloidin staining revealed that LAT-A markedly reduced F-actin expression, and Y27632 decreased the expression of cortical F-actin, resulting in a loss of cell–cell adhesion (Fig. 4E). Correspondingly, these inhibitors significantly decreased the cortical expression of E-cad and ZO-1 (Fig. 4F and G). qRT-PCR analysis revealed that *E-cad* mRNA was significantly decreased by Y27632, but not by LAT-A (Fig. 4H). In contrast, *ZO-1* mRNA expression was modestly increased by Y27632 and LAT-A (Fig. 4I).

4. Discussion

We demonstrated that both LPA_6 and LPA producing enzymes including PA-$PLA_1\alpha$ and ATX are more expressed in M-ABs than in other ameloblast-lineage cells, suggesting that LPA-LPA_6 signaling is distinctly functional in M-ABs, and PA-$PLA_1\alpha$ and ATX-induced LPA acts on LPA_6 in an autocrine/paracrine manner. Consistent with our results, previous studies have demonstrated that PA-$PLA_1\alpha$ induced LPA_6-mediated signaling in hair follicles in an autocrine/paracrine manner [10]. Additionally, since M-ABs are in contact with papillary layers containing rich blood vessels on the proximal side, this is likely to enable an abundant supply of ATX and LPA from the blood to the proximal end of M-ABs. Indeed, our present study showed that LPA_6 was strongly expressed at proximal end of M-ABs, and in LPA_6 KO mice, active RhoA expression was prominently reduced in the proximal side of M-ABs. Further, active RhoA was induced on the side facing the culture media containing LPA *in vitro*; thus, suggesting that LPA-LPA_6 signal at proximal side predominantly contributes to the regulation of M-ABs.

Herein, we have shown that cell morphology and polarity in M-ABs are markedly perturbed in LPA_6 KO mice. Additionally, analysis of LPA_6 KO mice and *in vitro* study using LPA_6 siRNA revealed that LPA-LPA_6 signaling modulates the expression and localization of E-cad, ZO-1, and F-actin, which are components of the cell junctional complex. These molecules are involved in maintaining epithelial cell polarity, in establishing structurally and functionally distinct apical and basal-lateral domains, and in recruiting signaling proteins for various cellular functions [24]. During enamel maturation, the establishment of cell morphology and polarity of M-ABs is essential for exerting necessary functions [12,25]. Therefore, our results strongly suggest that LPA-LPA_6 signaling plays a crucial role in the establishment of cell morphology and polarity by ensuring junction formation and actin organization for the proper functioning of M-ABs and thereby, enamel mineralization.

We showed that RhoA mediates LPA_6-induced cell–cell junction and actin cytoskeleton, indicating that RhoA signaling plays a pivotal role in the development and functioning of M-ABs. A detailed study was performed showing that knockdown of LPA_6 and RhoA inhibition suppressed E-cad both at the mRNA and the protein levels. In turn, F-actin inhibition suppressed E-cad at the protein level, but not at the mRNA level. These results suggest that LPA_6-RhoA signaling regulates the transcription of E-cad in a F-actin-independent manner, and stabilized E-cad protein in the cell membrane by anchoring it to F-actin as previously shown [26]. Inhibition of LPA_6, RhoA, and F-actin also suppressed ZO-1 protein expression in the cellular membrane, while slightly increasing its transcription. These results suggest that LPA_6-RhoA-F-actin axis stabilized the ZO-1 protein in the cell membrane. However, there may be unknown compensatory transcriptional mechanisms that counteract the loss of ZO-1 protein.

In this study, we showed the contribution of LPA-LPA_6-RhoA signaling axis to M-ABs regulation. This discovery not only has significant impacts on our understanding of the regulatory mechanism underlying normal amelogenesis but also raises the possibility that failure of this signaling cascade can cause enamel abnormalities in human patients. Although homozygous mutations in the PA-$PLA_1\alpha$ and LPA_6 genes are implicated in a congenital hair disorder, no enamel abnormalities have been reported in the patients [7,8,27]. Since the dental findings in those reports were obtained largely from macroscopic observations, it is unclear how the genetic abnormality of LPA_6 signaling affects the minute physical characteristics of the enamel. Thus, a detailed oral examination and tooth analysis of those patients can provide some clarification. To date, various causal genes of inherited enamel defects, such as amelogenesis imperfecta, have been identified. These genes are involved in diverse functions [13]; however, the involvement of LPA_6 signal-related genes with amelogenesis imperfecta has not yet been shown. Additionally, it was recently suggested that a combination of environmental factors and mutations in multiple genes cause anhidrotic ectodermal dysplasia and molar incisor hypomineralization [28,29]. Therefore, further studies to clarify whether the abnormality of LPA-LPA_6-RhoA signaling-related genes causes enamel defect, either as a single contributor or by interacting with

other genes and environmental factors, will aid in developing novel diagnostic, treatment, and prevention strategies for those diseases.

5. Conclusion

This study demonstrated that LPA-LPA$_6$ signaling is essential for establishing proper cell morphology and polarity of M-ABs responsible for enamel mineralization. We have mechanistically demonstrated that LPA-LPA$_6$ signaling activates RhoA, which in turn promotes the expression and stability of cell junctional proteins and cortical actin cytoskeleton (Fig. 4J). These results present a novel role of a bioactive lipid in teeth and attempt to elucidate the regulatory mechanism of tooth mineralization.

Ethical approval

All animal experiments were conducted in compliance with ARRIVE guidelines. The protocol for experimentation was approved by the Institutional Animal Care and Use Committee (Approval no. 23–065, 26–045, 2016PhA-022) and the Institutional Recombinant DNA Experiments Safety Committee of Iwate Medical University and Tohoku University (Approval no. 329, 442, 581, 2015PhLMO-011).

CRediT authorship contribution statement

Akira Inaba: literature search, figure, Methodology, data collection, data analysis, data interpretation, writing. **Hidemitsu Harada:** literature search, figure, Methodology, data collection, data analysis, data interpretation, critically revised manuscript. **Shojiro Ikezaki:** data collection, data analysis, data interpretation, critically revised manuscript. **Mika Kumakami-Sakano:** data collection, data analysis, data interpretation, critically revised manuscript. **Haruno Arai:** data collection, data analysis, data interpretation, critically revised manuscript. **Marii Azumane:** data collection, data analysis, data interpretation, critically revised manuscript. **Hayato Ohshima:** data collection, data analysis, data interpretation, critically revised manuscript. **Kazumasa Morikawa:** data interpretation, critically revised manuscript. **Kuniyuki Kano:** data interpretation, critically revised manuscript. **Junken Aoki:** data interpretation, critically revised manuscript. **Keishi Otsu:** literature search, figure, Methodology, data collection, data analysis, data interpretation, writing.

Conflicts of interest

The authors declare no competing financial interests.

Acknowledgments

We thank T. Fukasawa, T. Sugawara, W. Yashuno, M. Takahashi (Center for In Vivo Science in Iwate Medical University), and Aya Kikuchi (Division of Developmental Biology and Regenerative Medicine, Department of Anatomy, Iwate Medical University) for providing technical assistance, and Yukiko Onuma and Michiko Sugawara (Division of Developmental Biology and Regenerative Medicine, Department of Anatomy, Iwate Medical University) for their secretarial support. This work was financially supported by JSPS KAKENHI (grant numbers: 21K09832 and 18K09526 to KO, 16K15813 to HH), JSPS and NRF under the Japan-Korea Basic Scientific Cooperation Program (2018–2020), and KEIRYOKAI Research grant (Collaborative project 2017–2019).

Appendix A. Supplementary data

Supplementary data to this article can be found online at https://doi.org/10.1016/j.job.2022.01.004.

References

[1] Moolenaar WH, van Meeteren LA, Giepmans BN. The ins and outs of lysophosphatidic acid signaling. Bioessays 2004;26:870–81.
[2] Aikawa S, Hashimoto T, Kano K, Aoki J. Lysophosphatidic acid as a lipid mediator with multiple biological actions. J Biochem 2015;157:81–9.
[3] Kihara Y, Mizuno H, Chun J. Lysophospholipid receptors in drug discovery. Exp Cell Res 2015;333:171–7.
[4] Aoki J, Inoue A, Okudaira S. Two pathways for lysophosphatidic acid production. Biochim Biophys Acta - Mol Cell Biol Lipids 2008;1781:513–8.
[5] Choi JW, Herr DR, Noguchi K, Yung YC, Lee C-W, Mutoh T, et al. LPA receptors: subtypes and biological actions. Annu Rev PharmacolToxicol 2010;50:157–86.
[6] Pasternack SM, von Kügelgen I, Al Aboud K, Lee Y-A, Rüschendorf F, Voss K, et al. G protein–coupled receptor P2Y5 and its ligand LPA are involved in maintenance of human hair growth. Nat Genet 2008;40:329–34.
[7] Shimomura Y, Wajid M, Ishii Y, Shapiro L, Petukhova L, Gordon D, et al. Disruption of P2RY5, an orphan G protein–coupled receptor, underlies autosomal recessive woolly hair. Nat Genet 2008;40:335–9.
[8] Kazantseva A, Goltsov A, Zinchenko R, Grigorenko AP, Abrukova AV, Moliaka YK, et al. Human hair growth deficiency is linked to a genetic defect in the phospholipase gene LIPH. Science 2006;314:982–5.
[9] Shimomura Y, Wajid M, Petukhova L, Shapiro L, Christiano AM. Mutations in the lipase H gene underlie autosomal recessive woolly hair/hypotrichosis. J Invest Dermatol 2009;129(Issue 3):622–8.
[10] Inoue A, Arima N, Ishiguro J, Prestwich GD, Arai H, Aoki J. LPA-producing enzyme PA-PLA1α regulates hair follicle development by modulating EGFR signalling. EMBO J 2011;30:4248–60.
[11] Bartlett JD. Dental enamel development: proteinases and their enamel matrix substrates. ISRN Dent 2013;2013:24. https://doi.org/10.1155/2013/684607. 684607.
[12] Nanci A. Ten cate's oral histology. 7 edn. Elsevier; 2008.
[13] Smith CE, Poulter JA, Antanaviciute A, Kirkham J, Brookes SJ, Inglehearn CF, et al. Amelogenesis imperfecta; genes, proteins, and pathways. Front Physiol 2017;8:435.
[14] Heasman SJ, Ridley AJ. Mammalian Rho GTPases: new insights into their functions from in vivo studies. Nat Rev Mol Cell Biol 2008;9:690–701.
[15] Popoff MR, Geny B. Multifaceted role of Rho, Rac, Cdc42 and Ras in intercellular junctions, lessons from toxins. Biochim Biophys Acta 2009;1788:797–812.
[16] Riento K, Ridley AJ. Rocks: multifunctional kinases in cell behaviour. Nat Rev Mol Cell Biol 2003;4:446–56.
[17] Otsu K, Kishigami R, Fujiwara N, Ishizeki K, Harada H. Functional role of rho-kinase in ameloblast differentiation. J Cell Physiol 2011;226:2527–34.
[18] Otsu K, Ida-Yonemochi H, Ikezaki S, Ema M, Hitomi J, Ohshima H, et al. Oxygen regulates epithelial stem cell proliferation via RhoA-actomyosin-YAP/TAZ signal in mouse incisor. Development 2021;148:dev194787. https://doi.org/10.1242/dev.194787.
[19] Kawano S, Morotomi T, Toyono T, Nakamura N, Uchida T, Ohishi M, et al. Establishment of dental epithelial cell line (HAT-7) and the cell differentiation dependent on Notch signaling pathway. Connect Tissue Res 2002;43:409–12.
[20] Makishi S, Saito K, Ohshima H. Osteopontin-deficiency disturbs direct osteogenesis in the process of achieving osseointegration following immediate placement of endosseous implants. Clin Implant Dent Relat Res 2017;19:496–504.
[21] Sonoda H, Aoki J, Hiramatsu T, Ishida M, Bandoh K, Nagai Y, et al. A novel phosphatidic acid-selective phospholipase A1 that produces lysophosphatidic acid. J Biol Chem 2002;277:34254–63.
[22] Aoki J, Taira A, Takanezawa Y, Kishi Y, Hama K, Kishimoto T, et al. Serum lysophosphatidic acid is produced through diverse phospholipase pathways. J Biol Chem 2002;277:48737–44.
[23] Otsu K, Ida-Yonemochi H, Fujiwara N, Harada H. The semaphorin 4D-RhoA-akt signal cascade regulates enamel matrix secretion in coordination with cell polarization during ameloblast differentiation. JBone Miner Res 2016;31:1943–54.
[24] Drubin DG, Nelson WJ. Origins of cell polarity. Cell 1996;84:335–44.
[25] Lacruz RS, Habelitz S, Wright JT, Paine ML. Dental enamel formation and implications for oral health and disease. Physiol Rev 2017;97:939–93.
[26] Engl W, Arasi B, Yap LL, Thiery JP, Viasnoff V. Actin dynamics modulate mechanosensitive immobilization of E-cadherin at adherens junctions. Nat Cell Biol 2014;16:584–91.
[27] Horev L, Saad-Edin B, Ingber A, Zlotogorski A. A novel deletion mutation in P2RY5/LPA6 gene cause autosomal recessive woolly hair with hypotrichosis. J Eur Acad Dermatol Venereol 2010;24:858–9.
[28] Garot E, Rouas P, Somani C, Taylor GD, Wong F, Lygidakis NA. An update of the aetiological factors involved in molar incisor hypomineralisation (MIH): a systematic review and meta-analysis. Eur Arch Paediatr Dent 2021. https://doi.org/10.1007/s40368-021-00646-x.
[29] Suzuki T, Tajima H, Migita M, Pawankar R, Yanagihara T, Fujita A, et al. A case of anhidrotic ectodermal dysplasia presenting with pyrexia, atopic eczema, and food allergy, Asia Pac. Allergy 2019;9. https://doi.org/10.5415/apallergy.2019.9.e3.